https://erjm.journals.ekb.eg
ISSN: 1110-1180

DOI: ---------

ERJ
Engineering Research Journal
Faculty of Engineering
Menoufia University

Numerical Investigation on Reinforced Concrete Closed Curved Beams Subjected to Internal Pressure Strengthened with Sustainable Materials

Ahmed A. Hamoda[1], Boshra Eltaly[2], Mohamed S. Ghalla[1,3,*]

[1]Civil Engineering Dept., Faculty of Engineering, Kafrelsheikh University, Kafrelsheikh, Egypt
[2]Civil Engineering Dept., Faculty of Engineering Menoufia University, Egypt
[3]M. Sc. Candidate, Civil Engineering Dept., Faculty of Engineering Menoufia University, Egypt
**(Corresponding author: Mohamed_Shabaan@eng.kfs.edu.eg)*

ABSTRACT
This numerical study presents a Finite Element Modeling (FEM) for Closed Curved Beams (CCBs). This study aims to capture the effect of Stainless-Steel Layers (SSLs) and Engineered Cementitious Composites (ECC) as sustainable strengthening materials on the structural performance of RC CCBs under pressure loads. The numerical analysis was implemented using Abaqus and validated against previous experimental results. A parametric study and a numerical validation for RC CCBs strengthened with SSLs and ECC were conducted using 18 beams divided into 5 groups. The main studied parameters were: number/layout of SSLs with varied thicknesses and ECC layer with varied thicknesses and configuration. The structural behaviour was improved by the SSLs numbers and thicknesses were increased. The cracking load was improved by about 16-43% for studied SSLS groups and the ultimate capacity was significantly increased by about 29-66%. The elastic stiffness was enhanced by 1.2-4.1 times higher than the unstrengthen beam. The effect of ECC layer was studied. The cracking was improved by increasing the thicknesses by about 18-25%. The ultimate capacity was significantly increased by about 56-76%. The elastic stiffness was enhanced by about 1.4-3.3 times higher than the master beam.

Keywords: *closed curved beams; Engineered cementitious composite; stainless steel layers; Strengthening techniques; Finite element modeling.*

1. Introduction

Strengthening of reinforced concrete (RC) structures are often required due to the aging of structures, increasing the service loads, or improving the ductility of structures. Such strengthening can be achieved by several techniques, such as: enlarging the concrete member employing flowable high-performance concrete (HPC) with higher ductility, using external bonded fiber-reinforced polymer or steel plates as an additional reinforcement [1-6].

Strengthening of RC beams is commonly used for enhancing shear and flexural capacities [7,8]. Numerous Studies have been carried out in this type of strengthening. However, very limited researches focused on improving structured exhibition of RC Closed Curved Beams (CCBs) in particular with presence of ring tensile forces employing sustainable techniques .

RC CCBs are widely used in mosques, churches, circular tanks, and concrete silos used to collect oil. Such beams have the same stresses of ordinary beams but tensile stresses are the major one. Unlike the flexural failure with ductile mode for common RC beams located in maximum moment zone, tension failure may be generated with a more ductile appearance and cracks distributed along the beam. Such failure may be attributed to the slower propagation of vertical and diagonal cracks as a result of excessive ring tensile stresses [9].

Dong et al. [10] carried out an experimental investigation on mechanical behaviour of ECC ring beam connections under square local compressive loading. The results showed that, increasing the width of CCBs resulted in a significant increase in the horizontal displacement ductility. These results confirm the great advantages of the use of ECC in the ring beam connections.

The width and reinforcement ratios had different effects on the main performance of the ECC ring beams. Increase them produced a positive effect on the initial cracking load and the width ratio had the most impact. The reinforcement ratio had the greatest influence on ultimate capacity [11]. For the energy dissipation, the width ratio had a dominant effect on

the behaviour of the energy dissipation, and the energy dissipation increased by 3 times for ring beams with large heights [12]. Ren et al [13] studied the seismic performance of a ring beams. The influence of the beam reinforcement ratio and axial force ratio on the deceleration curve, ultimate load, ductility and dissipated energy were significant. The strain analysis of RC column with ring beam joint under axial compression was examined experimentally by Feng et al [14].

Certainly, tensile stresses greatly affect the normal types of concrete that do not contain fibers. Therefore, the tensile stresses must all be attributed to the reinforcement with neglecting the slight effect of the NC [15-17]. Modeling and characterization of strengthened concrete tension members were studied by Hansen and Henrik [18]. The behaviour of the strengthening elements under the influence of tensile stresses in the RC beams improves the performance of the elements well[19] .

Using Stainless Steel Layers (SSLs) is new and innovative, and it has become a good option due to the use of SSLs material and its mechanical properties. SSLs have favorable mechanical properties due to its high strength and ductility [20]. Experimental and numerical investigations of stainless-steel tubular columns were studied by Al-Osta et al [21]. It can be found that the common mode of failure for such SS columns is local buckling failure. For stainless steel columns having circular sections, outward local buckling failure occurs close to the column ends. Kavitha et al [22] studied theoretically the flexural and compressive behaviour of I steel section strengthened by SSLs. SS application shows distinctive mechanical characteristics compared to steel, such as rounded stress–strain relationship, significant strain hardening and high ductility. It is well suited for impact resistant structures, fire, explosion resistant walls, seawalls, piers, coastal structures and structures under aggressive environment [27].

Guo and Chan [23] studied theoretically the stainless-steel ring strengthened removable dowel bar connection system. As usual, stainless steel gave better results and had a clear effect on the overall behavior of the element after strengthening. The concrete that confining with stainless-steel tubes as well as the presence of vertical SS stiffeners seemed to have a significant reflection on enhancing elastic–plastic performance and the total capacity [24, 25]. Hamoda et al. [26] carried out an experimental and numerical investigations of the effectiveness of Engineered Cementitious Composites (ECC) and SSLs in shear strengthening of reinforced concrete beams .

The presence of ECC layers as strengthening strategy showed a ductile failure mode with a large number of hair cracks at early loading stage. The strengthening technique employing ECC and SSLs significantly enhances the total capacity of RC beams by 20-60% .

ECC has been recently used as one of the new High-Performance Concretes (HPCs) that can be applied for RC structural strengthening. Unlike the NC, the ECC has several advantages including higher flowability, best strain-hardening, excellent durability, large number of cracks, and crack narrow width [28-32]. The application of ECC as strengthening mix was studied by Shan et al. [33]. In this technique, ECC acts as both a matrix for bonding and a new cover replacing the damaged concrete. An experimental investigation of corrosion-damaged RC beams strengthened in flexure with ECC layer was conducted by Shan et al. [34]. Due to its superior ductility and strain hardening performance, ECC was examined as flexural and shear strengthening techniques [35-38]. The shear strengthening of RC beams with FRP grid-reinforced ECC matrix was studied by Wan-Yang et al. [39]. As expected, the presence of the ECC gave a lot of endurance to the elements used. Shear strengthening of RC short columns with ECC jacket was examined experimentally by Zhang et al. [40]. The perfect performance of the ECC covered columns was significantly improved compared with the master one, which was characterized by plumper and more hysteresis loops with good improved plastic deformation capacity. Mingke et al. [41] carried out an experimental investigation on strengthening of flexure-dominate RC members with ECC cover. The ECC It is considered one of the most important types of concrete used in strengthening at the present time.

There is a lack and uncertainty regarding application of sustainable material. Stainless Steel (SS) is the popular sustainable material that available to strengthen RC elements. Due to its superior ductility and significant resistance to corrosions, SS is proposed in this study as a high tensile material combined as a tension strengthening technique .

The current numerical study aimed to study the structural behavior of RC CCBs strengthened with SSLs and ECC layer. Two numerical models were developed and validated by the results from the previous published experimental work carried out by Dong et al. [10]. Then, a parametric study was conducted to evaluate different strengthening techniques used to improve the tension stresses in RC CCBs. The First was strengthening by External Bonded Reinforcement (EBR) by using outer SSLs. Twelve models divided into three groups were selected to study the application of SSLs. The main studied parameter herein, the number/layout and thicknesses of SSLs. The thicknesses of 0.60, 0.80, 1.00, and 1.25 mm were studied. One, two, and three SSLs were chosen for first, second, and third group, respectively. The application of ECC as strengthening

strategy was studied in order to enhance the ring action of RC CCBs. Six models divided into two groups were selected with two studied parameters, configuration and thickness of layer, and studied analytically. The thicknesses of 15, 20, and 25 mm were studied. The horizontal displacement values corresponding to the cracking and ultimate stages (Δcr) and (Δu), respectively were compared. The numerical outcomes were: load-displacement behavior, cracking loads (Pcr), ultimate capacities (Pu), elastic stiffness (K), and absorbed energy (E). Theses outcomes were chosen to be compared with the master CCB in order to capture the main enhancement in ring action.

2. The Considered Previous Experimental Study

Dong et al. [10] carried out an experimental investigation on the mechanical behavior of ECC ring beam connections that applied to ring tension stresses as shown in Figure. 1(a) .

In this published experimental study, the constraint performance of the continuous beams was not included, and hence the main and transverse reinforcements in the connected beam and column were neglected when designing the specimens in the experiments. The local compressive behavior can be clearly evaluated by the ring tension stresses that generated due to the horizontal displacement. The steel stirrups and ring steel reinforcements were used inside the encircling CCBs. The steel stirrups with 6 mm diameter were spaced at 30◦ intervals along the circumferential steel ring bars, as shown in Figure. 1(b). All CCBs were tested under the ring action behaviour. A total of 15 CCB connection specimens with various studied parameters were selected and prepared. The application of ECC at these specimens were conducted. Three CCB specimens were prepared with the same studied parameters (width, height and reinforcement ratio) as the ECC CCB connections.

Twelve ECC CCBS were prepared to study the effect of the width factor (a = w/d), height-to-width ratio (b = h/w) and reinforcement ratio (c = As/(w×h)). In this regard, d represents the inner diagonal length of the CCB, h and w are the height and width of the beam, respectively, and As denotes the area of the ring steel bars of the CCB section. The geometric details and reinforcement of the two chosen CCBs from this study are shown in Figure. 2. The notation of the CCB specimens is as follows: The first character of the notation “C” or “E” represents the matrix material of concrete or ECC, respectively.

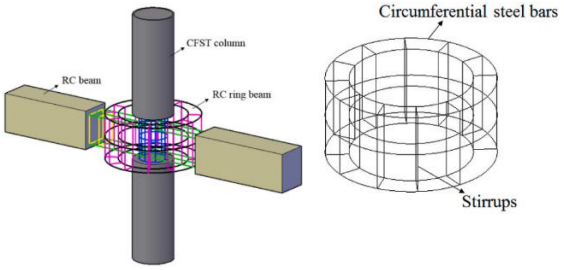

(a) (b)

Figure 1- RC CCBs; (a) Schematic diagram, and (b) Reinforcement details [10].

From previous experimental study [10], the first considered spacemen was the NC CCB that named (C-A2B1C2) where C represents normal concrete, A2 represents 0.47 width factor, B1 represents 1% height-to-width ratio, and reinforcement ratio of 2%. This CCB was selected to be compared with the ECC one. The geometric details and reinforcement of this specimens were shown in in Figure. 2. Two types of ring steel bars were used. The upper was two bars with 10 mm diameter and the bottom were one with 10 mm diameter and one with 8 mm diameter. All CCBs were surrounded by 6 mm stirrups located at every equal angle of 30º. The second considered specimen was the ECC CCB that named (E-A2B1C2) where E represents ECC, A2 represents 0.47 width factor, B1 represents 1% height-to-width ratio, and reinforcement ratio of 2%. This CCB was selected to be compared with the NC one in order to evaluate the enhancement ratio for structural performance. The geometric details and reinforcement of this specimen were identical to the first chosen one as shown in Figure. 2.

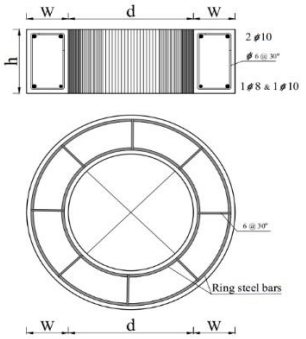

Figure 2- Geometric details and reinforcement for NC and ECC CCB.

3. Preparation and Creation of Numerical Model.

Three-dimensional Finite Element Model (FEM) for RC CCBs was developed using program Abaqus [42]. The first and second FEMs were developed considering material properties and geometric parameters of published previous experimental work in RC CCBs specimens that examined experimentally

by Dong et al. [10]. The FEM results were then validated against those captured in the previous experimental work in terms of load-displacement response, cracking and mode of failures. These terms were used to validate the FEM. After the model was validated, it was used to conduct a parametric study on sustainable strengthening techniques available for RC CCBs. These techniques were EBR SSLs and EBR ECC layer with wide variation in studied parameters.

3.1. Constitutive Modeling of Materials and Sensitivity of Numerical Parameters

NC and ECC were the two concrete materials that were introduced in this research. The Concrete Damage Plasticity (CDP) model was selected for defining the plastic mechanical behavior of concrete due to the ability to simulate deterioration that caused by cracking and nonlinear deformation in compression and tension.

The CDP model is available in the Abaqus package as shown in Figure 3 [43]. The material constitutive models of the first CCB material under compressive and tension stresses are depicted in Figure 4 (a and b), respectively. The compression stress–strain relationships were developed using the formulas proposed by Aslani [48] as shown in Figure 4. It is worth to mentioning that, the tension performance (stress–strain law) of NC has been presented as a linear behavior up to the maximum value that obtained using the tensile test as recommended by Aslani [48] as shown in Figure 4(b). Then, the tensile stress was reduced down to zero. Unlike the first type NC, which presents a sudden deterioration beyond the linear stage, the second ductile ECC behaves multiple cracks with large strain-hardening. Compressive and tensile stress–strain laws of the ECC were given by many researchers [44-47]. The constitutive laws of the ECC that were adopted in this numerical research were employed in compression as shown in Figure 5(a) and tension as shown in Figure 5(b).

Several Finite Element Models (FEMs) were executed in order to study the sensitivity and capturing the best constitutive parameters required to correctly describe the CDP model specified for the both NC and ECC. Such parameters are dilation angle (ψ), viscosity relaxation parameter (μ), eccentricity (e), the ratio of biaxial to uniaxial compressive yield stresses (f_{bo}/f_{co}), the ratio of the second stress invariant on the tensile to the compressive meridian (K_c). The K_c value ranged in between 0.65 and 0.85 [49-51]. while satisfying results were observed with the default value of 0.68 in Abaqus [56-58].

The ratio of f_{bo}/f_{co} ranged in between 1.10 and 1.16 according to the previous study conducted by Jin et al [52]. The acceptable validation was obtained for a value of 1.16. The eccentricity value was used as a default of 0.1. Several trails with different viscosity parameters varied as follows 0.00, 0.0001, 0.0005, 0.0008, 0.0009, and 0.001. The sensitivity of numerical results with zero value, as recommended by Eurocode [52]. From several FEMs with different dilation angles ranging in between 10 and 55, the acceptable results were founded for an angle of 35 for ECC and NC as recommended by Meng et al [53]. The Poisson's ratios of steel, NC, and ECC were chosen as 0.3, 0.2, and 0.22, respectively. In addition, unlike the concrete smeared cracking design option founded in ABAQUS where shear retention needs to be specified, the CDP model chosen in this study can appropriately yield the tensile behavior of concrete elements through the tensile damage that available in the software. Reinforcing steel bars and stirrups were modeled using a linearly elastic-plastic model as shown in Figure 4(c). Linear behavior represents the elastic stage up to the yield point. The second followed linear stage by hardening behavior respecting to plastic stage up to ultimate load. Three used steel bars were modeled. Three ring steel bars with 10 mm diameter and one with 8 mm diameter. The stirrups diameter was 6 mm mild steel.

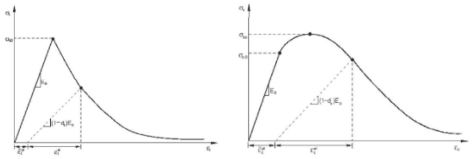

(a) (b)

Figure 3- CDP model provided by Abaqus [43]; (a) Tension, and (b) Compression.

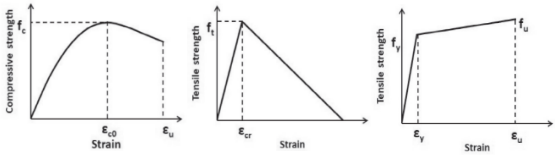

(a) (b) (c)

Figure 4- Materials constitutive models used in FEM for NC [48]; (a) Concrete in compression, (b) Concrete in tension, and (c) Steel.

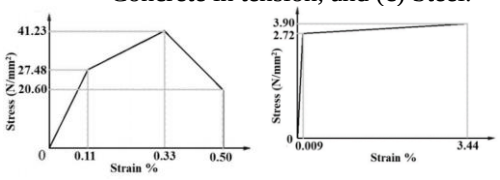

(a) (b)

Figure 5- Materials constitutive models used in FEM for ECC; (a) ECC in compression, and (b) ECC in tension [44-47, 55].

3.2. Model Set-up

The main elements of the FEMs were concrete (NC and ECC) and steel bars. Two models were prepared and studied herein in order to validate the used FEM. The solid continuum formula was used to model the

RC CCBs, while wire elements used for model the steel bars. The model utilized the three-dimensional and eight-node linear hexahedral solid elements with reduced integration (C3D8R) to simulate RC CCB geometry, in conjunction three-dimensional, two-node, truss elements (T3D2) in ABAQUS software to simulate steel bars and stirrups. The model set-up can be seen in Figure 6(a). The reinforcing steel bars and stirrups elements and arrangement were shown in Figure 6(b). For the lower surface of modeled beams, only vertical movement is prohibited and movement in all directions is allowed. This was done to simulate the movement of joints in space in the same way. Loading was carried out on the inner surface of the models with the forces of internal pressure, as it happens due to the vertical loads located on the connections, which are transformed into lateral displacements in the curved beams. These boundary conditions were shown in Figure 6(a). Figure 6 shows view of the developed FEM for beam (C-A2B1C2), and beam (E-A2B1C2), respectively. The two beams have the same dimensions and the same reinforcement, but the difference was in the type of concrete only. The first is NC while the second is ECC.

Perfect interaction between reinforcing steel bars/stirrups and the used two concretes was assumed to create the interaction between steel bars and concrete. This assumption was achieved using embedded element constraint available in ABAQUS software. In such constraint, steel bars were selected to be embedded in the concrete beam as a host region. The surface area of the inner surface of the RC CCBs was determined in order to calculate the total force acting on the beams in cracking and ultimate stages. The total force was calculated by multiplying the internal pressure stress applied to it by the area. For the two samples, the same loading rate was used with a different final load value. Then the total load was calculated for both stages.

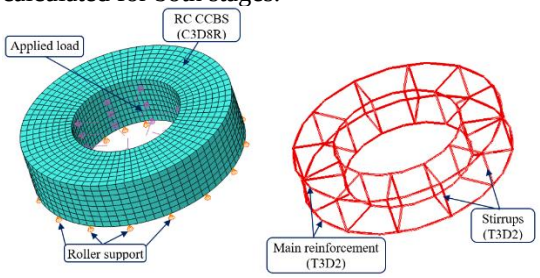

(a) (b)

Figure 6- Model set-up: (a) Concrete elements type, loading, and boundary condition, and (b) Types of steel elements.

3.4. FEM Validation

published previous experimental [10] versus FEMs results were studied and discussed in this section. The load- displacement responses for the two CCBs are presented in Figure 7. For the two beams: (C-A2B1C2) and (E-A2B1C2), FEM results showed nearly similar results to those obtained experimentally. However, a more pronounced deviation, in the ultimate stage, was observed in case of beam E-A2B1C2 that was formed from ECC. Additionally, the effect of the ratio of steel reinforcement and height to width ratio were almost similar when compared to published previous experimental results showing that the FEM was able to reasonably predict the behavior of RC CCBs in terms of load capacity, load-horizontal displacement curves and mode of failure. Numerical results and previous experimental ones are compared and analyzed to verify the rationality and accuracy of the established model and the FEM results. It is worth to mention that these results were very similar. With the difference in the type of concrete used in each beam, the proper representation of the samples helped in these results.

In this context, the crack patterns obtained through the FEM are compared to those obtained experimentally and presented in Figure 8.

Because of the high tensile ductility and excellent crack width control ability of the ECC components, there were large numbers of cracks at the outer side as shown in Figure 8(b). In addition, the crack width in the ECC beam can be controlled to a small value, which is useful to reduce the penetration of water or oils and hence increase the structural durability. On another side, the NC CCB had the same failure mode but with a few numbers of cracks as shown in Figure 8(b).

In the ultimate stage, severe concrete spalling occurred for RC beams connections, whereas the ECC beam connection achieved a good integrity. This difference in the failure mode is due to the bridging action of the internal fibers and compatible deformation between the ring steel bars and ECC.

For the first case study beam C-A2B1C2, first cracks appeared at the outer side of the CCB with vertical appearance as shown in Figure 8(a) at a total load of about 1724 kN [10] and 1812 kN (Numerical) with 5.1% variation ratio in cracking stage. With further loading, crack width increased and other cracks spread on the outer side till the cracks appeared at the inner side. The FEM peak load was 2539 kN and the published previous experimental capacity was 2387 kN with 6.3% variation ratio in peak load.

Load-deflection response for second beam was shown in Figure 7(b), elastic linear stage ended at a total load of about 2105 kN (previous experimental) and 2293 kN (Numerical) with 8.9% variation ratio in initial stage. With the load increase, crack width increased and other cracks spread on the outer tension side till the cracks distributed encircling the whole concrete section. The FEM ultimate load was 2974 kN and the

published previous experimental load was 2857 kN with 4.1% variation ratio in plastic stage.

There was more validation in terms of yield and ultimate displacement. The yield displacement for first beam was about 3.7 mm (previous experimental) 3.5 mm (Numerical) with 5.4% variation ratio. The yield displacement for ECC beam was about 3.4 mm (previous experimental) 3.2 mm (Numerical) with 6.2% variation ratio.

The ultimate displacement for first beam was about 11.9 mm (previous experimental) 10.1 mm (Numerical) with 17.8% variation ratio. The ultimate displacement for ECC beam was about 17.1 mm (previous experimental) 16.0 mm (Numerical) with 6.8% variation ratio.

FEMs results showed satisfied correlation between published previous experimental and FEM results with an available variation in elastic and plastic stage, respectively. This numerical model may be satisfied model of the suitable trials performed to simulate the RC CCBs and its strengthening techniques. This model with the same parameter will used in the followed parametric study on application of SSLs and ECC layers as strengthening techniques that available for RC CCBs.

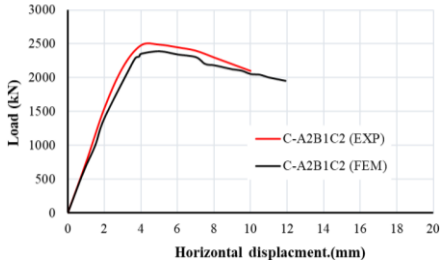

(a)

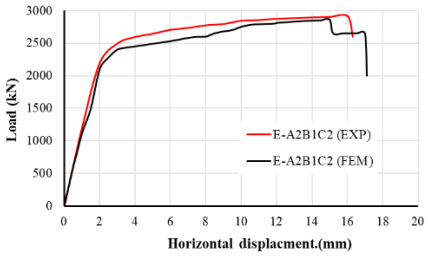

(b)

Figure 7- Load-deflection relationships that obtained experimentally by published previous work [10] and numerically: (a) beam (C-A2B1C2), and (b) beam (E-A2B1C2).

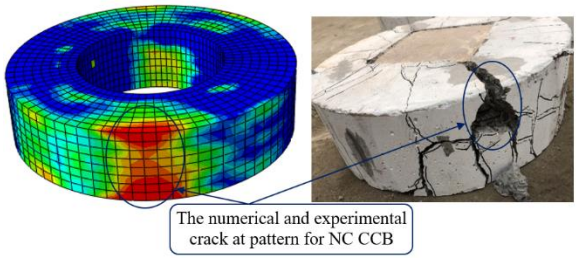

(a)

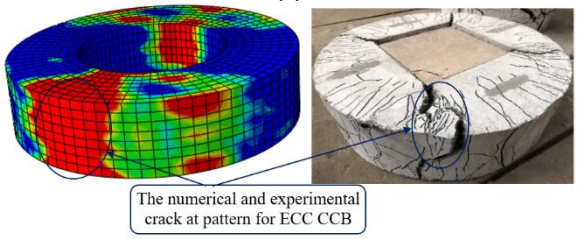

(b)

Figure 8- Crack pattern and failure modes: (a) beam (C-A2B1C2), and (b) beam (E-A2B1C2).

3.5. Parametric Study on Strengthening of CCBs with SSLs and ECC

RC CCBs is an essential element of water and oil tanks, and many other different shell structures. These structures, some of which represent aesthetic members, while others represent strategic one. Recently, during the service-life of these RC structures, there is an inevitable need for strengthening of their members to enhance the ultimate capacity and to satisfy serviceability.

These structures are often subjected to continuous tensile stresses. Therefore, the use of strengthening techniques that preserve the section and its external dimensions is the best option. EBR system is the most suitable one that is able to enhance structural behavior of such beams. This technique enables improving the mechanical properties of the elements without compromising their basic body.

This study aimed to study the behavior of RC CCBs strengthened by SSLs and ECC layers under tension stresses. The parametric study was conducted by utilizing the validated FEMs. A detailed parametric study is carried out to evaluate the effects of application of SSLs, number and lay out of SSLs, and thicknesses of SSLs. The second strengthening technique was the application of covering ECC layer. A total of 18 CCBs divided into five groups were studied numerically up to failure. The groups and their studied parameters are tabulated in Table 1. All studied beams were constructed with an identical geometric properties and reinforcement details as shown in Figure 9. All studied large scale beams had 2400mm outer diameter and 2000mm inner diameter with 600mm height. The first group consisted of four

CCBs strengthened by one SSL with 200 mm width as shown in Figure 9(a) and Table 1. The thicknesses of 0.60, 0.80, 1.0, and 1.25 mm were studied for beams B-NC-SS-1-0.6, B-NC-SS-1-0.8, B-NC-SS-1-1.0, and B-NC-SS-1-1.25, respectively.

The second group consisted of four CCBs strengthened by two SSLs with 100 mm width as shown in Figure 9(b) and tabulated in Table 1. The thicknesses of 0.60, 0.80, 1.0, and 1.25 mm were studied for beams B-NC-SS-2-0.6, B-NC-SS-2-0.8, B-NC-SS-2-1.0, and B-NC-SS-2-1.25, respectively. The third group consisted of four CCBs strengthened by three SSLs with 100 mm width as shown in Figure 9(c) and tabulated in Table 1. The thicknesses of 0.60, 0.80, 1.0, and 1.25 mm were studied for beams B-NC-SS-3-0.6, B-NC-SS-3-0.8, B-NC-SS-3-1.0, and B-NC-SS-3-1.25, respectively. The master beam without strengthening was concluded to all groups in order to be compared.

The ECC layers was selected to study its effect on structural performance of RC CCBs as EBR strengthening technique. Two groups were studied, the fourth group and the fifth one. The main object herein is to find the best configuration to the covering ECC layer. Three beams were studied in each group with variable layer thickness.

The fourth group consists of three CCBs strengthened by outer vertical ECC layer that covers the whole vertical outer side of the beam with 600 mm width as shown in Figure 9(d) and tabulated in Table 1. The thicknesses of 15, 20, and 25 mm were studied for beams B-ECC-1-15, B-ECC-1-20, and B-ECC-1-25, respectively.

The fifth group consists of three CCBs strengthened by outer vertical and horizontal ECC layer that cover the whole outer three sides of the beam as shown in Figure 9(e) and tabulated in Table 1. The thicknesses of 15, 20, and 25 mm were studied for beams B-ECC-3-15, B-ECC-3-20, and B-ECC-3-25, respectively. The main output of this study is to compare the enhancement due to the strengthening in the cracking and ultimate stages, elastic stiffness, and absorbed energy. All strengthened CCBs were studied on the same validated FEM.

The fourth group consists of three CCBs strengthened by outer vertical ECC layer that covers the whole vertical outer side of the beam with 600 mm width as shown in Figure 9(d) and tabulated in Table 1. The thicknesses of 15, 20, and 25 mm were studied for beams B-ECC-1-15, B-ECC-1-20, and B-ECC-1-25, respectively.

The fifth group consists of three CCBs strengthened by outer vertical and horizontal ECC layer that cover the whole outer three sides of the beam as shown in Figure 9(e) and tabulated in Table 1. The thicknesses of 15, 20, and 25 mm were studied for beams B-ECC-3-15, B-ECC-3-20, and B-ECC-3-25, respectively. The main output of this study is to compare the enhancement due to the strengthening in the cracking and ultimate stages, elastic stiffness, and absorbed energy. All strengthened CCBs were studied on the same validated FEM.

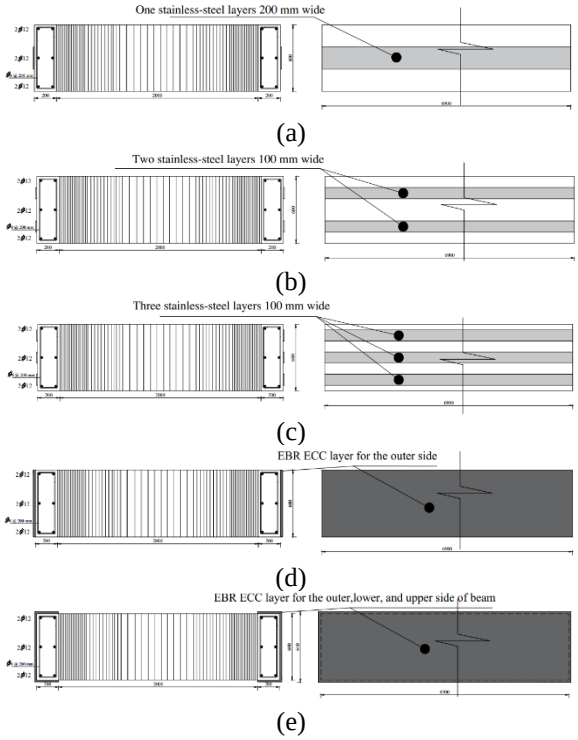

Figure 9- Geometric details for strengthened groups: (a) Group G1, (b) Group G2, (c) Group G3, (d) Group G4, and (e) Group G5.

The details of the FEMs that were used in this parametric study in terms of element types, boundary conditions, loading, and interactions is shown in this section. The continuum, three-dimensional and eight-node linear hexahedral solid elements with reduced integration (C3D8R) in ABAQUS was used to model the concrete of CCBs (NC and ECC) as shown in Figure 10(a). The reinforcement ring steel bars and closed stirrups were defined using the two-node and linear truss elements (T3D2) as shown in Figure 10(b). Four-node shell element with reduced integration (S4R) was employed to simulate the SSLs that used for EBR strengthening technique as shown in Figure 10(a). The boundary conditions were concluded the loading and supporting system. The model was supported on 3d roller supports selected in lower side of beams. The loads were applied as pressure load distributed uniformly on the inner side of CCBs. These loading and boundary conditions are shown in Figure 10(a).

The interaction between the steel bars/stirrups and concrete was simulated using tie interaction.

Table 1- Test matrix.

Group	Specimen`s ID	Concrete type	Strengthening technique	Number of Layers	Thickness
G1	B-NC	NC	EBR using SSLs	--------	--------
	B-NC-SS-1-0.6	NC		1 Laver	0.6 mm
	B-NC-SS-1-0.8	NC		1 Layer	0.8 mm
	B-NC-SS-1-1.0	NC		1 Layer	1.00 mm
	B-NC-SS-1-1.25	NC		1 Layer	1.25 mm
G2	B-NC	NC	EBR using SSLs	--------	--------
	B-NC-SS-2-0.6	NC		2 Layers	0.8 mm
	B-NC-SS-2-0.8	NC		2 Layers	1.00 mm
	B-NC-SS-2-1.0	NC		2 Layers	1.25 mm
	B-NC-SS-2-1.25	NC		2 Layers	1.50 mm
G3	B-NC	NC	EBR using SSLs	--------	--------
	B-NC-SS-3-0.6	NC		3 Layers	0.8 mm
	B-NC-SS-3-0.8	NC		3 Layers	1.00 mm
	B-NC-SS-3-1.0	NC		3 Layers	1.25 mm
	B-NC-SS-3-1.25	NC		3 Layers	1.50 mm
G4	B-NC	NC	Covering with ECC layer	--------	--------
	B-ECC-1-15	ECC		One side	15 mm
	B-ECC-1-20	ECC		One side	20 mm
	B-ECC-1-25	ECC		One side	25 mm
G5	B-NC	NC	Covering with ECC layer	--------	--------
	B-ECC-3-15	ECC		Three sides	15 mm
	B-ECC-3-20	ECC		Three sides	20 mm
	B-ECC-3-25	ECC		Three sides	25 mm

In the tie technique, the concrete beam was the host region while the truss elements representing the reinforcement bars/stirrups were selected as the embedded region. The interaction between the outer surface of RC CCBs and inner surface of SSLs was tie-surface to surface constrain between both sides. This modeling was the same as the basic model in this study after validation. The same test setup applied for all 18 FEMs.

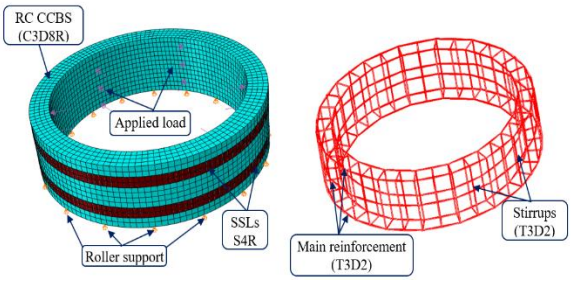

(a) (b)

Figure 10- Model set-up: (a) Types of elements, loading, and boundary condition, and (b) Types of steel elements.

The strengthened groups were studied in order to evaluate the best technique that able to increase the RC CCBs capacity and improve the whole structural behaviour. The setup of all studied groups can be seen in Figure 11. The SSLs durability performance makes it an interesting alternative for the structural strengthening of RC members.

The EBR technique is considered to be a cost-efficient alternative to replacing functionally deficient RC elements. For uncracked sections, the EBR can be applied to the soffit of RC members. Alternatively, it is common to use SSLs to offer high stiffness, strength, and directly bond to concrete surfaces with epoxy adhesive material. The application of SSLs as sustainable strengthening strategy is used herein as shown in Figure 11(a, b, and c) for groups G1, G2, and G3, respectively. The covering ECC layer was select as EBR strengthening strategy for these sections as shown in Figure 11(d and e) for groups G4 and G5, respectively.

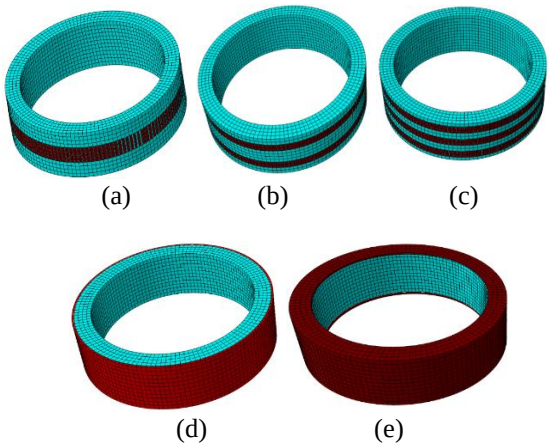

Figure 11- Model set-up for all groups: (a) Group G1, (b) Group G2, (c) Group G3, (d) Group G4, and (e) Group G5.

3.5.1. Effect of Application of EBR SSLs

One of the main objectives of this parametric study is the capture the effect of the SSLs on the tension behavior of the RC CCBs. The effect of four different SSLs thicknesses was investigated in this section. The details of the FEMs are presented in Table 1 and Figure 10. Three groups are considered with the same geometric RC details to evaluate the effect of SSLs thickness and arrangement in strengthening of RC CCBs. All these groups were strengthened with one, two, and three layers of SS for groups G1, G2, and G3, respectively. In the same group, the thickness of SSLs was variable. These thicknesses were: 0.60 mm, 0.80 mm, 1.00 mm, and 1.25 mm.

The results for these FEMs were compared with master beam (B-NC) to investigated the effect of ring SSLs thicknesses and layout. The numerical results for the FEMs for the three groups were tabulated in Table 2. The elastic stiffness index (K) and absorbed energy (E) were chosen to be compared for all strengthened beams as a clear indicator for comparison and determination of the behavior of RC beams. It was found that the new application of SSLs resulted in a better improvement in the E by about (1.93-2.23) times higher than those estimated from master beam. The numerical load-displacement curves of studied beams are depicted in Figure 12(a, b, c, d and e) for groups G1, G2, G3, G4, and G5, respectively. Table 2 shows the horizontal displacement values corresponding to the cracking and ultimate stages (Δcr) and (Δu), respectively. As an impression of the linear exhibition, the K estimated as the slope of the linear curve is provided in Table 2. It was found that the application of SSLs resulted in a better enhancement in the K by about (2.2-4.1) times higher than those estimated from master beam.

In fact, the presence of SSLs enhanced the load-displacement performance, cracking loads, ultimate loads, elastic stiffness, and absorbed energy. The crack pattern of the studied numerical CCBs was very close to those of validated beams. These stresses and cracks are shown in Figure 13. The outer side of all studied beams was the critical one because of the appearance of the first crack. Vertical cracks appeared at early loading stage at the outer side of CCBs and increase by loading as shown in Figure 13(a). Finally, and just before failure, the SSLs were fully stressed by tension stresses as shown in Figure 13(a and b).

3.5.2. Effect of Number and Lay-out of SSLs

The layout effect of SSLs and their numbers with the same thickness on the structural performance of RC CCBs strengthened in tension under static internal pressure loading was investigated by varying the layout of them. The -studied beams that strengthened by SSLs were divided into three groups. The studied number of layers were: one, two, and three layers for groups G1, G2, and G3, respectively.

The main obvious reflection of the layout of outer ring SSLs is represented in the area exposed to the strengthening in each group. Increasing the number with maintaining the same area may give better results due to the uniform distribution of tension loads and the good bond for each layer. In the case of deep beams, it is preferable to distribute the stresses on a larger number of strengthening layers. The number of SSLs represents an increase in the total cracking and ultimate capacity of the beams.

Fig. 12 shows the load–displacement for these three groups of beams. All CCBs exhibited a linear behavior up to the cracking load with the same performance. Beyond that, a gradual change in the slope of the load–displacement relationship was observed. Then, the pressure was increased, the yielding of the internal ring steel reinforcement occurred in all specimens, while the manifested load–displacement plateaus after yielding were varied according to the strengthening techniques. The structural performance was improved by the SSLs numbers were increased. The cracking load was improved by about 39%, 42%, and 43% for groups G1, G2, and G3, respectively as shown in Table 2. The ultimate capacity was significantly increased by about 53%, 57%, and 66% for groups G1, G2, and G3, respectively. Moreover, the elastic stiffness was enhanced by 2.2, 3, and 4.1 times higher than the master CCB for groups G1, G2, and G3, respectively as tabulated in Table 2.

It is clear that, increasing the number of SSLs more than two layers per 0.6 meter improves the structural behavior. It is worth mentioning that the use of one strip every 0.6 meter is not suitable for this type of beams. The uniform distribution of the SSLs on the

surface exposed to the strengthening increases the efficiency of the layers and their uniform behavior with the CCBs as shown in Figure 13.

3.5.3. Effect of Thicknesses of SSLs

The reflection of the SSLs thickness studied in this numerical study was also investigated on the tension performance of the RC CCBs in order to find the optimum strengthening strategy to save cost and to present full information about the best technique for CCBs. Three different FEMs groups were designed with a similar thickness of 0.60, 0.80, 1.00, and 1.25 mm but with different number of layers.

One layer of SS selected for the first group G1 in the specimens: B-NC-SS-1-0.6, B-NC-SS-1-0.8, B-NC-SS-1-1.0, and B-NC-SS-1-1.25 were studied. The increase of SSLs thickness improves the cracking load by about 16-39%. The ultimate capacity was significantly increased by about 29-53%. The elastic stiffness was enhanced by about 1.25-2.22 times higher than the unstrengthen CCB. The cracking load was improved by the increase of SSLs thicknesses by about 18-42%. The ultimate capacity was significantly increased by about 35-57%. The elastic stiffness was enhanced by about 1.3-3 times higher than the master beam as shown in Table 2.

For the third group G3 the specimens: B-NC-SS-3-0.6, B-NC-SS-3-0.8, B-NC-SS-3-1.0, and B-NC-SS-3-1.25 were studied. The cracking load was improved by the increase of SSLs thicknesses by about 19-43%. The ultimate capacity was significantly increased by about 49-66%. The elastic stiffness was enhanced by about 1.3-4.1 times higher than the master beam as shown in Table 2. Figure 13(a and b) shows the all stresses and crack pattern for studied beams that strengthened by SSLs. The first crack appeared at outer side of CCBs with vertical appearance while the SSLs was fully stressed and began to failure as shown in Figure 13(a). There were many vertical cracks appeared parallel to the initial one distributed along the outer side. The failure modes for all studied beams were tension failure governed by SSLs rupture at the maximum stressed zone as shown in Figure 13(b).

The main structural behavior of this type of strengthening is the tensile behavior of smooth steel bars. Because most of the tensile stresses are borne by the steel elements only because the lower tensile capacity of normal concrete. External strengthening with SSLS in an annular shape parallel to the reinforcing steel bars increases the efficiency of the beams while preserving the structural behavior.

3.5.4. Effect of Application of EBR ECC Layer

The ECC layer as strengthening technique has several advantages including higher flowability, higher strain-hardening, significant durability, tighter cracks, and crack width control. In this

technique, a thin cover layer of ECC is applied to sustain and uniformly distribute the tension stress along the outer side of CCBS. The ductile performance of ECC will then disperse the distributed stress through bridging fibres so that it forms multiple fine cracks. Preserving the concrete section, especially in water structures, is very important. Adding a thin layer of ECC with different thickness to the outer surface of CCBs is a good technique to strengthening this type of beams. The all-studied beams that strengthened by ECC layer were divided into two groups with varied thickness. The thicknesses were: 15, 20, and 25 mm for groups G4 and G5.

The fourth group aims to study the effect of one vertical ECC layer as shown in Figure 11(d). This layer was studied as EBR strengthening strategy for one side. In addition, the fifth group aims to study the effect of three ECC layers for vertical and two horizontal sides as shown in Figure 11(e).

3.5.5. Effect of Thickness of ECC Layer

For the fourth group G4 the specimens: B-ECC-1-15, B-ECC-1-20, and B-ECC-1-25 were studied. The cracking load was improved by the increase ECC thicknesses by about 16-23%. The ultimate capacity was significantly increased by about 44-57%. The elastic stiffness was enhanced by about 1.26-3.13 times higher than the master beam as shown in Table 2. Figure 13(c, b, and d) shows the all stresses and crack pattern for studied beams that strengthened by ECC. The initial cracks appeared at outer side of CCBs with vertical appearance while the ECC layer began to withstand tensile stresses faster than the CCB as shown in Figure 13(c). There were many vertical cracks appeared parallel to the initial one distributed along the outer side. The ECC covered all outer sides of CCB in fifth group G5 the specimens: B-ECC-3-15, B-ECC-3-20, and B-ECC-3-25 were studied. The cracking was improved by the increase the thicknesses by 18-25%. The ultimate capacity was significantly increased by about 56-76%. The elastic stiffness was enhanced by about 1.4-3.3 times higher than the master beam as shown in Table 2. The crack pattern for three sides ECC beams can be seen in Figure 13(d). The main note her in that, ECC layer began to withstand tensile stresses faster than the CCB especially the upper and lower one as shown in Figure 13(d and e). The cracks generated from outer to inner side as shown in Figure 13(e).

Table 2- Numerical results.

Gro.	Specimen ID	Cracking Stage			Ultimate Stage			Elastic Stiffness Index (K)	K_B/K_0	Absorbed Energy (E)
		Pcr (kN)	PcrB/ PcrB0	Δcr (mm)	Pu (kN)	PuB/ PuB0	Δ_u (mm)			
G1	B-NC	352	1.00	0.43	503	1	5.1	818.6	1	2744
	B-NC-SS-1-0.6	410	1.16	0.40	652	1.29	6.5	1025.0	1.25	4043
	B-NC-SS-1-0.8	456	1.29	0.36	712	1.41	6.8	1266.6	1.55	4479
	B-NC-SS-1-1.0	482	1.36	0.31	740	1.47	7.1	1554.8	1.90	4892
	B-NC-SS-1-1.25	490	1.39	0.27	770	1.53	7.3	1814.8	2.22	5292
G2	B-NC	352	1.00	0.43	503	1	501	818.6	1	
	B-NC-SS-2-0.6	418	1.18	0.38	680	1.35	6.5	1100.0	1.34	4209
	B-NC-SS-2-0.8	461	1.31	0.35	740	1.47	7.3	1317.1	1.61	4777
	B-NC-SS-2-1.0	485	1.37	0.29	770	1.53	7.3	1672.4	2.04	5167
	B-NC-SS-2-1.25	502	1.42	0.20	790	1.57	7.6	2510.0	3.07	5718
G3	B-NC	352	1.00	0.43	503	1	5.1	818.6	1	
	B-NC-SS-3-0.6	422	1.19	0.37	752	1.49	7.8	1140.5	1.39	4893
	B-NC-SS-3-0.8	465	1.32	0.30	775	1.54	8	1550.0	1.89	5368
	B-NC-SS-3-1.0	490	1.39	0.24	800	1.59	8.2	2458.3	3.00	5678
	B-NC-SS-3-1.25	505	1.43	0.15	840	1.66	8.4	3366.6	4.11	6127
G4	B-NC	352	1.00	0.43	503	1	5.1	818.6	1	
	B-ECC-1-15	411	1.16	0.40	729	1.44	4.1	1027.5	1.26	2660
	B-ECC-1-20	421	1.19	0.28	760	1.51	4.4	1503.5	1.84	3093
	B-ECC-1-25	435	1.23	0.17	790	1.57	4.8	2558.8	3.13	3325
G5	B-Nc	352	1.00	0.43	503	1	5.1	818.6	1	
	B-ECC-3-15	418	1.18	0.35	789	1.56	4.5	1194.2	1.46	3312
	B-ECC-3-20	435	1.23	0.21	839	1.66	4.8	2071.4	2.53	3529
	B-ECC-3-25	442	1.25	0.16	889	1.76	5	2762.5	3.37	3724

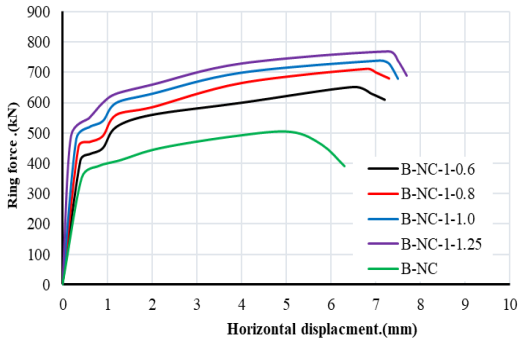

(a)

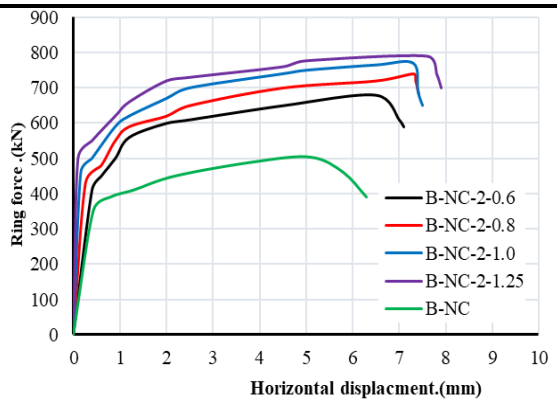

(b)

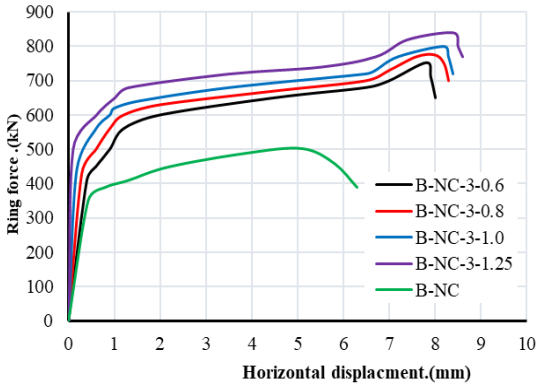

(c)

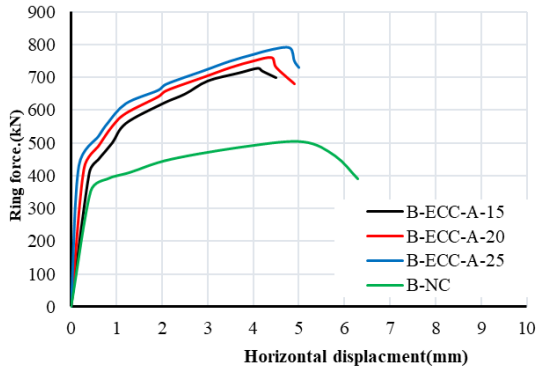

(d)

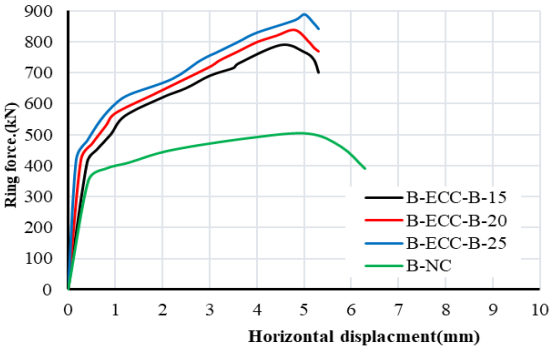

(e)

Figure 12- Load-displacement relationships obtained Numerically: (a) Group G1, (b) Group G2, (c) Group G3, (d) Group G4, and (e) Group G5.

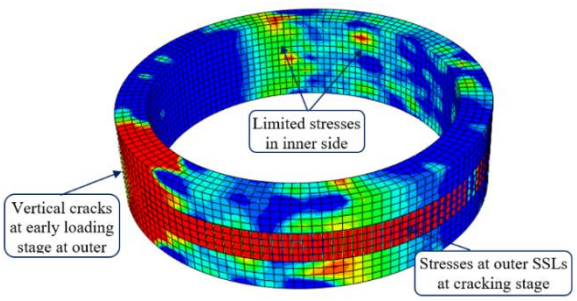

(a)

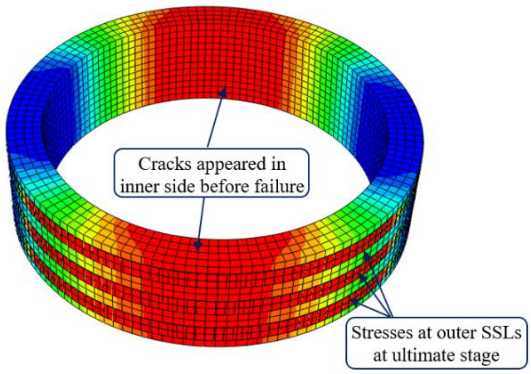

(b)

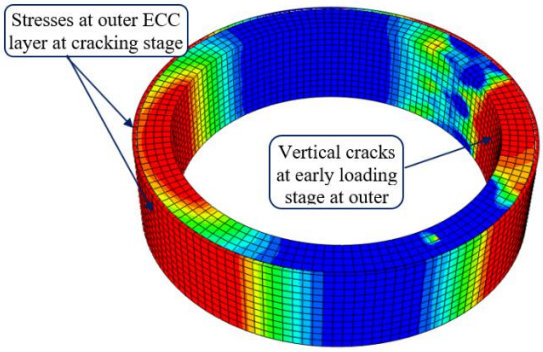

(c)

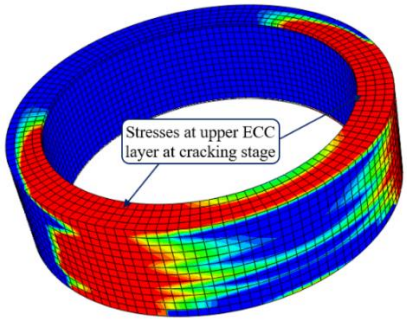

(d)

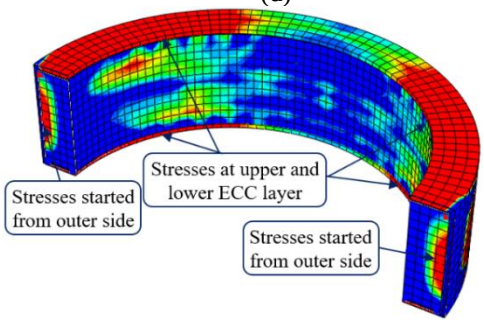

(e)

Figure 13- Numerical results (Crack pattern and stresses): (a) Early loading stage for SSLs groups, (b) Just before failure for SSLs groups, (C) Early loading stage for ECC groups, (d) stresses at ECC layer, and (e) stresses and cracks of ECC groups.

4. Conclusions

This numerical study presents the numerical simulation and analysis of RC CCBs strengthened by two techniques. EBR SSLs and EBR ECC covering layer were studied. The studied beams were subjected to static internal pressure loading through FEMs. The FE modelling were validated by selecting two CCBs connections that examined experimentally at previous experimental work [10] and then comparing the FE results with those from selected experimental work. Results from this study implied that this FEM is able to simulate the RC CCBs and its strengthening. A parametric study was performed to evaluate the effects of SSLs and ECC on the structural performance of the modelled beams under applied loads. The major observations of this research can be captured as follows:

1. The FEM can effectively predict the main behavior of RC CCBs strengthened with SSLs and ECC layer as sustainable material subjected to applied loads. The application of SSLs and ECC as strengthening technique showed a better structural behavior.
2. The structural behavior was improved by increasing SSLs numbers. The cracking load was improved by about 16-43% for examined groups. The ultimate capacity was significantly increased by about 29-66% for these groups and the elastic stiffness was enhanced by 1-4 times higher than the master beam.
3. The investigation of the effect of the SSLs thicknesses on the tension behavior of the CCBs was the main objective. The cracking and ultimate loads were improved by increasing the layers thicknesses by about 43% and 66%, respectively.
4. Adding ECC layer as cover strengthening technique improved cracking and ultimate loads by about 25% and 76%, respectively. using of three layers credit the best enhancement for ECC beams.

5. References

[1] Mercimek, Ö., Ghoroubi, R., Özdemir, A., Anil, Ö., & Erbaş, Y. (2022). Investigation of strengthened low slenderness RC column by using textile reinforced mortar strip under axial load. Engineering Structures, 259, 114191.

[2] Saeed, Y. M., Aules, W. A., & Rad, F. N. (2022). Post-strengthening rapid repair of damaged RC columns using CFRP sheets for confinement and NSM-CFRP ropes for flexural strengthening. In Structures (Vol. 43, pp. 1315-1333). Elsevier.

[3] Yoo, D. Y., Chun, B., Oh, T., Jang, Y. S., & Lee, J. H. Strengthening Effect of Concrete Beams Using Ultra-Rapid-Hardening Fiber-Reinforced Mortar Under Flexure. Available at SSRN 413079.

[4] Sun, P., Hou, X., Zheng, W., & Cao, S. (2022). Strengthening of conventional columns through RPC sandwich tube against blast loading. In Structures (Vol. 45, pp. 1850-1863). Elsevier.

[5] Zhang, Y., Wang, L., & Li, X. (2022, October). Strengthening of overloaded PRC beams with the combination of CFRP laminates bonding and resin injection. In Structures (Vol. 44, pp. 72-83). Elsevier.

[6] Li, R., Deng, M., Chen, H., & Zhang, Y. (2022, October). Shear strengthening of RC shear-deficient beams with highly ductile fiber-reinforced concrete. In Structures (Vol. 44, pp. 159-170). Elsevier.

[7] Selvapriya, R., Kumar, V. A., Keruthiga, V., Kumar, A. M., & Bharath, G. (2022). Experimental investigation on the behaviour of flexural strengthening of beams using carbon fibre reinforced polymer sheet. Materials Today: Proceedings.

[8] Moubarak, A. M., Elwardany, H., El-hassan, K. A., & Taher, S. E. D. (2022). Shear strengthening of wide-shallow beams by inserted fasteners. Engineering Structures, 268, 114554.

[9] Song, Z., Yu, F., Zhang, N., & Fang, Y. (2021). A model for predicting load-displacement hysteretic behavior of PVC-CFRP confined concrete column-ring beam interior joints under low cyclic loading. Composite Structures, 265, 113769.

[10] Dong, B., Pan, J., Cai, J., & Ozbakkaloglu, T. (2021). Mechanical behavior of ECC ring beam connections under square local compressive loading. Journal of Building Engineering, 34, 101741.

[11] Dong, B., Pan, J., Cai, J., & Zeng, H. (2020, October). Experimental study on local compressive behaviour of ECC ring beam connections. In Structures (Vol. 27, pp. 2069-2081). Elsevier.

[12] Dong, B., Pan, J., & Xu, L. (2022). Numerical and theoretical analysis of beam-to-column connections with ECC ring beams subjected to local compression loading. Journal of Building Engineering, 52, 104466.

[13] Ren, F. M., Tian, S. Y., Gong, L., Wu, J. L., Mo, J. X., Lai, C. L., & Lai, M. H. (2022). Seismic performance of a ring beam joint connecting FTCES column and RC/ESRC beam with NSC. Journal of Building Engineering, 105366.

[14] Yu, F., Zhang, N., Niu, D., Kong, Z., Zhu, D., Wang, S., & Fang, Y. (2019). Strain analysis of PVC-CFRP confined concrete column with ring beam joint under axial compression. Composite Structures, 224, 111012.

[15] Kwak, H. G., & Kim, D. Y. (2006). Cracking behavior of RC panels subject to biaxial tensile stresses. Computers & structures, 84(5-6), 305-317.

[16] Shabdin, M., Zargaran, M., & Attari, N. K. (2018). Experimental diagonal tension (shear) test of Un-Reinforced Masonry (URM) walls strengthened with textile reinforced mortar (TRM). Construction and building materials, 164, 704-715.

[17] Cui, L., Zhang, X., Hao, H., & Kong, Q. (2022). Improved resistance functions for RC elements accounting for compressive and tensile membrane actions. Engineering Structures, 251, 113549.

[18] Hansen, C. S., & Stang, H. (2012). Modeling and characterization of strengthened concrete tension members. Engineering Fracture Mechanics, 82, 85-99.

[19] Hansen, C. S., & Stang, H. (2012). Modeling and characterization of strengthened concrete tension members. Engineering Fracture Mechanics, 82, 85-99.

[20] Sharif, A. M., Al-Mekhlafi, G. M., & Al-Osta, M. A. (2019). Behavior of circular stainless steel stub columns internally strengthened by longitudinal carbon steel bars. Engineering Structures, 199, 109617.

[21] Al-Mekhlafi, G. M., Al-Osta, M. A., & Sharif, A. M. (2020). Experimental and numerical investigations of stainless steel tubular columns strengthened by CFRP composites. Thin-Walled Structures, 157, 107080.

[22] Kavitha, R., Sundarraja, M. C., Indhiradevi, P., Manikandan, P., Karthikeyan, G., Rahman, A. A., & Akash, E. (2022). Flexural and compressive behaviour of I steel section strengthened by stainless steel plate. Materials Today: Proceedings, 52, 351-354.

[23] Guo, J., & Chan, T. M. (2022, October). Stainless steel ring strengthened removable dowel bar connection system: Effect of key parameters and design recommendations. In Structures (Vol. 44, pp. 1767-1782). Elsevier.

[24] Islam, S. Z., Cai, Y., & Young, B. (2019). Design of CFRP-strengthened stainless steel tubular sections subjected to web crippling. Journal of Constructional Steel Research, 159, 442-458.

[25] Hamoda, A., Abdelazeem, F., & Emara, M. (2021). Concentric compressive behavior of hybrid concrete–stainless steel double-skin tubular columns incorporating high performance concretes. Thin-Walled Structures, 159, 107297.

[26] Hamoda, A., Ahmed, M., & Sennah, K. (2022). Experimental and numerical investigations of the effectiveness of engineered cementitious composites and stainless steel plates in shear strengthening of reinforced concrete beams. Structural Concrete.

[27] Lalthazuala, R., & Singh, K. D. (2019). Investigations on structural performance of hybrid stainless steel I-beams based on slenderness. Thin-Walled Structures, 137, 197-212.

[28] Lye, H. L., Mohammed, B. S., Liew, M. S., Wahab, M. M. A., & Al-Fakih, A. (2020). Bond behaviour of CFRP-strengthened ECC using Response Surface Methodology (RSM). Case Studies in Construction Materials, 12, e00327.

[29] Wu, C., & Li, V. C. (2017). CFRP-ECC hybrid for strengthening of the concrete structures. Composite Structures, 178, 372-382.

[30] Hu, B., Zhou, Y., Xing, F., Sui, L., & Luo, M. (2019). Experimental and theoretical investigation on the hybrid CFRP-ECC flexural strengthening of RC beams with corroded longitudinal reinforcement. Engineering Structures, 200, 109717.

[31] Sharbatdar, M. K., & Tajari, A. (2021). Experimental in-plane seismic strengthening of masonry infilled reinforced concrete frames by engineered cementitious composites (ECC). Construction and Building Materials, 293, 123529.

[32] Guo, R., Ren, Y., Li, M., Hu, P., Du, M., & Zhang, R. (2021). Experimental study on flexural shear strengthening effect on low-strength RC beams by using FRP grid and ECC. Engineering Structures, 227, 111434.

[33] Na, L., Wangpeng, L., Yiyan, L., & Shan, L. (2022). Corroded reinforced concrete columns strengthened with basalt fibre reinforced ECC under axial compression. Composite Structures, 116328.

[34] Zheng, A., Liu, Z., Li, F., & Li, S. (2021). Experimental investigation of corrosion-damaged RC beams strengthened in flexure with FRP grid-reinforced ECC matrix composites. Engineering Structures, 244, 112779.

[35] Hou, W., Li, Z. Q., Gao, W. Y., Zheng, P. D., & Guo, Z. X. (2020). Flexural behavior of RC beams strengthened with BFRP bars-reinforced ECC matrix. Composite Structures, 241, 112092.

[36] Zheng, Y. Z., Wang, W. W., & Brigham, J. C. (2016). Flexural behaviour of reinforced concrete beams strengthened with a composite reinforcement layer: BFRP grid and ECC. Construction and Building Materials, 115, 424-437.

[37] Li, Z. Q., Hou, W., & Lin, G. (2021). Flexural strengthening of RC beams with BFRP or high strength steel bar–reinforced ECC matrix.

Construction and Building Materials, 303, 124404.

[38] Zheng, A., Li, S., Zhang, D., & Yan, Y. (2021). Shear strengthening of RC beams with corrosion-damaged stirrups using FRP grid-reinforced ECC matrix composites. Composite Structures, 272, 114229.

[39] Yang, X., Gao, W. Y., Dai, J. G., & Lu, Z. D. (2020). Shear strengthening of RC beams with FRP grid-reinforced ECC matrix. Composite Structures, 241, 112120.

[40] Deng, M., Zhang, Y., & Li, Q. (2018). Shear strengthening of RC short columns with ECC jacket: Cyclic behavior tests. Engineering Structures, 160, 535-545.

[41] Zhang, Y., Deng, M., Li, T., & Dong, Z. (2021). Strengthening of flexure-dominate RC columns with ECC jackets: Experiment and analysis. Engineering Structures, 231, 111809.

[42] ABAQUS/CAE.: Finite Element Analysis Program Version 6.14-3.(2017) .

[43] Lezgy-Nazargah, M., Dezhangah, M., & Sepehrinia, M. (2018). The effects of different FRP/concrete bond-slip laws on the 3D nonlinear FE modeling of retrofitted RC beams-A sensitivity analysis. Steel and Composite Structures, 26(3), 347-360.

[44] Ge, W. J., Ashour, A. F., Ji, X., Cai, C., & Cao, D. F. (2018). Flexural behavior of ECC-concrete composite beams reinforced with steel bars. Construction and Building Materials, 159, 175-188.

[45] Ma, H., Zhang, Z., Ding, B., & Tu, X. (2018). Investigation on the adhesive characteristics of Engineered Cementitious Composites (ECC) to steel bridge deck. Construction and Building Materials, 191, 679-691.

[46] Ge, W., Ashour, A. F., Cao, D., Lu, W., Gao, P., Yu, J., ... & Cai, C. (2019). Experimental study on flexural behavior of ECC-concrete composite beams reinforced with FRP bars. Composite Structures, 208, 454-465.

[47] Wu, C., & Li, V. C. (2017). CFRP-ECC hybrid for strengthening of the concrete structures. Composite Structures, 178, 372-382.

[48] Aslani, F. (2016). Mechanical properties of waste tire rubber concrete. Journal of Materials in Civil Engineering, 28(3), 04015152.

[49] Hamoda, A., & Hossain, K. M. A. (2019). Numerical assessment of slab–column connection additionally reinforced with steel and CFRP bars. Arabian Journal for Science and Engineering, 44(10), 8181-8204.

[50] Lubliner, J., Oliver, J., Oller, S., & Oñate, E. (1989). A plastic-damage model for concrete. International Journal of solids and structures, 25(3), 299-326.

[51] Lee, J., & Fenves, G. L. (1998). Plastic-damage model for cyclic loading of concrete structures. Journal of engineering mechanics, 124(8), 892-900.

[52] Jin, H., Li, F., & Hu, D. (2022). Research on the flexural performance of reinforced engineered cementitious composite beams. Structural Concrete, 23(4), 2198-2220.

[53] Européen, C. (2004). Eurocode 2: Design of concrete structures—Part 1-1: General rules and rules for buildings. London: British Standard Institution.

[54] Ma, H., Zhang, Z., Ding, B., & Tu, X. (2018). Investigation on the adhesive characteristics of Engineered Cementitious Composites (ECC) to steel bridge deck. Construction and Building Materials, 191, 679-691.

[55] Ahmed, M., Liang, Q. Q., Hamoda, A., & Arashpour, M. (2022). Behavior and design of thin-walled double-skin concrete-filled rectangular steel tubular short and slender columns with external stainless-steel tube incorporating local buckling effects. Thin-Walled Structures, 170, 108552.

[56] Ci, J., Ahmed, M., Liang, Q. Q., Chen, S., Chen, W., Sennah, K., & Hamoda, A. (2022). Experimental and numerical investigations into the behavior of circular concrete-filled double steel tubular slender columns. Engineering Structures, 267, 114644.

[57] Hamoda, A., Elsamak, G., Emara, M., Ahmed, M., & Liang, Q. Q. (2023). Experimental and numerical studies of reinforced concrete beam-to-steel column composite joints subjected to torsional moment. Engineering Structures, 275, 115219.

[58] El-Mandouh, M. A., Elsamak, G., Abdelazeem, F., Hamoda, A., & Rageh, B. O. (2022). Experimental and Numerical Investigation of One-Way Reinforced Concrete Slabs Using Various Strengthening Systems. Case Studies in Construction Materials, e01691.